

Superconductivity of Rb_3C_{60} : breakdown of the Migdal-Eliashberg theory

E. Cappelluti^{1,a}, C. Grimaldi², L. Pietronero¹, S. Strässler², and G.A. Ummarino³

¹ Dipartimento di Fisica, Università “La Sapienza”, P.le A. Moro 2, 00185 Roma, and INFM Roma1, Italy

² École Polytechnique Fédérale de Lausanne, Département de Microtechnique IPM, 1015 Lausanne, Switzerland

³ INFM - Dipartimento di Fisica, Politecnico di Torino, c.so Duca degli Abruzzi 24, 10129 Torino, Italy

Received 30 March 2001

Abstract. In this paper, through an exhaustive analysis within the Migdal-Eliashberg theory, we show the incompatibility of experimental data of Rb_3C_{60} with the basic assumptions of the standard theory of superconductivity. For different models of the electron-phonon spectral function $\alpha^2F(\Omega)$ we solve numerically the Eliashberg equations to find which values of the electron-phonon coupling λ , of the logarithmic phonon frequency Ω_{ln} and of the Coulomb pseudopotential μ^* reproduce the experimental data of Rb_3C_{60} . We find that the solutions are essentially independent of the particular shape of $\alpha^2F(\Omega)$ and that, to explain the experimental data of Rb_3C_{60} , one has to resort to extremely large couplings: $\lambda = 3.0 \pm 0.8$. This result differs from the usual partial analyses reported up to now and we claim that this value exceeds the maximum allowed λ compatible with the crystal lattice stability. Moreover, we show quantitatively that the obtained values of λ and Ω_{ln} strongly violate Migdal’s theorem and consequently are incompatible with the Migdal-Eliashberg theory. One has therefore to consider the generalization of the theory of superconductivity in the nonadiabatic regime to account for the experimental properties of fullerenes.

PACS. 74.70.Wz Fullerenes and related materials – 74.20.-z Theories and models of superconducting state – 63.20.Kr Phonon-electron and phonon-phonon interaction

1 Introduction

In contrast to the cuprates, the other family of high- T_c superconductors, the fullerene compounds, shows a quite more conventional phenomenology: their normal state properties are Fermi liquid-like, no stripe formation or signal of pseudogap appear above T_c , they are s -wave superconductors with a sizeable carbon isotope effect [1]. It is certainly due to their apparently ordinary phenomenology that superconductivity in C_{60} materials is now often assumed to be correctly described by the conventional Migdal-Eliashberg (ME) theory of the electron-phonon driven superconductivity [2,3]. The relatively high critical temperatures of the A_3C_{60} fullerene compounds (up to $T_c^{\text{max}} = 40$ K for Cs_3C_{60} under pressure [4]) are therefore generally thought to be due to an optimized electron-phonon interaction achieved, according to the different proposed explanations, by a large electron coupling to the alkali phonons [5], to the C_{60} rotational modes [6], or by the so-called curvature argument for the intramolecular couplings [7,8]. According to this latter theory, the electron-phonon coupling steadily increases with the curvature of the fullerene molecule so that compounds with smaller molecular radius (C_{36} , C_{28}) are expected to have

critical temperatures even higher than those of the C_{60} -based materials [9].

The above theories disregard however several aspects of the phenomenology of the fullerene compounds which do not fit into the standard ME scenario. In fact, like the high- T_c copper-oxides, the fullerene compounds have extremely low charge carrier densities [10], have significant electron correlation [1,11], and are close to a metal-insulator transition [12,13] showing a strong dependence of T_c upon doping [14] and disorder [15]. From a ME point of view, these features tend to degrade the superconducting state so that it appears difficult to understand why the fullerene compounds should represent the best optimized ME materials.

In this situation, it should be therefore of primary importance to assess to which extent the experimental data can be explained by the ME theory. This issue has been even more highlighted by the recent discovery of superconductivity with $T_c = 52$ K in FET hole doped C_{60} [16]. Until recently, however, the spread of experimental results has prevented a detailed and definitive analysis. Nevertheless, in the last years, the experimental uncertainty for the alkali fullerene compound Rb_3C_{60} , which shows the highest critical temperature at room pressure $T_c = 30$ K within the A_3C_{60} family, has been considerably narrowed.

^a e-mail: emmcapp@pil.phys.uniroma1.it

In fact, resistive measurements on 99% enriched ^{13}C single-crystals have recently established the carbon isotope coefficient α_{C} with the best up-to-date accuracy, $\alpha_{\text{C}} = 0.21 \pm 0.012$ [17], resolving therefore a long standing uncertainty on the value of α_{C} in fullerenes mainly due to partial isotope substitution and/or magnetic measurements on powder samples with broad transitions often wider than the isotope shift itself [1,17]. In addition, crossed tunneling and optical transmission studies on the *same* sample have provided accurate measurements of the zero temperature energy gap 2Δ leading to $2\Delta/T_{\text{c}} = 4.2 \pm 0.2$ [18]. This result is more accurate than previous spectroscopic studies and agrees with NMR and photoemission measurements [19,20], moreover it has been obtained by both bulk- (optical transmission) and surface- (tunneling) sensitive measurements which have given often contrasting results.

Although we shall briefly consider also other estimations existing in literature, in this paper we mainly focus on the above reported experimental data. The main point in fact is that these data are supplemented by quite small error bars, which permit a more rigorous analysis. We shall show however that different determinations of the data, in particular of the superconducting gap, would even more subvert the results presented in this paper.

The experimental values above discussed seem, at first sight, perfectly compatible with the ME theory. For example, $T_{\text{c}} = 30$ K is not far from $T_{\text{c}} = 23.2$ K of Nb_3Ge and $2\Delta/T_{\text{c}} = 4.2 \pm 0.2$ is very close to 4.18 and 4.25 of V_3Ga and $\text{Nb}_3\text{Al}(2)$, respectively [21]. Finally, the carbon isotope coefficient $\alpha_{\text{C}} = 0.21$ is similar to the isotope effects of the elemental ME superconductors Os ($\alpha = 0.2$) and Mo ($\alpha = 0.33$) [22]. The apparently ordinary values of T_{c} , α_{C} , and $2\Delta/T_{\text{c}}$, independently considered, could therefore be used as arguments in favour of the validity of the ME theory for Rb_3C_{60} . However, each of these values has little meaning if taken individually. For example, in reference [18] the experimental data $T_{\text{c}} = 30$ K and $2\Delta/T_{\text{c}} = 4.2$, but not $\alpha_{\text{C}} = 0.21$, have been fitted by setting $\lambda = 1.16$, $\mu^* = 0.1$, and $\Omega_{\text{ln}} = 302$ K, while in reference [17] $T_{\text{c}} = 30$ K and $\alpha_{\text{C}} = 0.21$, but not $2\Delta/T_{\text{c}} = 4.2$, have been fitted by $\lambda = 0.9$, $\mu^* = 0.22$, and $\Omega_{\text{ln}} = 1360$ K. Although the discrepancies in the values of λ and μ^* are somehow acceptable, the two values of Ω_{ln} differ by a factor of five.

A previous partial analysis, based only on the values of the critical temperature $T_{\text{c}} = 30$ K and of the isotope coefficient $\alpha_{\text{C}} = 0.21$, has pointed out an intrinsic inconsistency of the ME framework with respect of the adiabatic assumption [23]. In this paper we extend this study by taking into account also the estimation of the superconducting gap $2\Delta/T_{\text{c}} = 4.2$ and by considering realistic electron-phonon interactions related both to inter- and intra- molecular modes. We show that the experimental data of Rb_3C_{60} , when analyzed in the context of the fullerene compounds, $T_{\text{c}} = 30$ K, $\alpha_{\text{C}} = 0.21$ and $2\Delta/T_{\text{c}} = 4.2$ are actually incompatible with the standard ME framework. We accomplish this task in Section 3 by considering different models of the electron-phonon

interaction and by numerically solving the ME equation in order to reproduce the experimental data. We find in Section 4 that the resulting values of the electron-phonon interaction are always far too large to avoid lattice instabilities and to neglect the electron-phonon vertex corrections beyond Migdal's limit, as required by the ME formulation [2,3]. Finally, in Section 5 we propose that the main origin of the failure of the ME framework lies in the breakdown of the adiabatic hypothesis (Migdal's theorem) which, in doped fullerenes, is naturally driven by the small value of the Fermi energy.

2 The Migdal-Eliashberg equations

As pointed out in the introduction, the superconducting state of the fullerene compounds is quite often regarded in terms of the ME theory. Since the alkali doped fullerenes are three dimensional *s*-wave superconductors, the superconducting properties are therefore thought to be correctly described by the standard ME equations [3,21]:

$$Z(i\omega_n) = 1 + \frac{\pi T}{\omega_n} \sum_m \int_0^\infty d\Omega \frac{\alpha^2 F(\Omega) 2\Omega}{\Omega^2 + (\omega_n - \omega_m)^2} \times \frac{\omega_m}{\sqrt{\omega_m^2 + \Delta(i\omega_m)}}, \quad (1)$$

$$Z(i\omega_n)\Delta(i\omega_n) = \pi T \sum_m \left[\int_0^\infty d\Omega \frac{\alpha^2 F(\Omega) 2\Omega}{\Omega^2 + (\omega_n - \omega_m)^2} - \mu \theta(\omega_c - |\omega_m|) \right] \frac{\Delta(i\omega_m)}{\sqrt{\omega_m^2 + \Delta(i\omega_m)}}. \quad (2)$$

In the above equations $Z(i\omega_n) = 1 - \Sigma(i\omega_n)/i\omega_n$, where $\Sigma(i\omega_n)$ is the normal state electronic self-energy, $\Delta(i\omega)$ is the Matsubara gap-function and ω_n and ω_m are Matsubara fermionic frequencies.

In the above equations, $\alpha^2 F(\Omega)$ is the electron-phonon spectral function (also known as the Eliashberg function) which defines the electron-phonon coupling constant λ and the logarithmic frequency Ω_{ln} through the following relations [21]:

$$\lambda = 2 \int \frac{d\Omega}{\Omega} \alpha^2 F(\Omega), \quad (3)$$

$$\ln \Omega_{\text{ln}} = \frac{2}{\lambda} \int \frac{d\Omega}{\Omega} \ln(\Omega) \alpha^2 F(\Omega). \quad (4)$$

The dimensionless parameter μ represents the effective Coulomb repulsion probed by the Cooper pair at the energy scale ω_c which is much larger than the phonon energy scale. It is clear that the value of the Coulomb parameter μ depends on the specific value of ω_c which is somewhat arbitrary [24]. In fact a more sound quantity is the pseudopotential μ^* defined as:

$$\mu^* = \frac{\mu}{1 + \mu \ln(\omega_c/\Omega_{\text{max}})}, \quad (5)$$

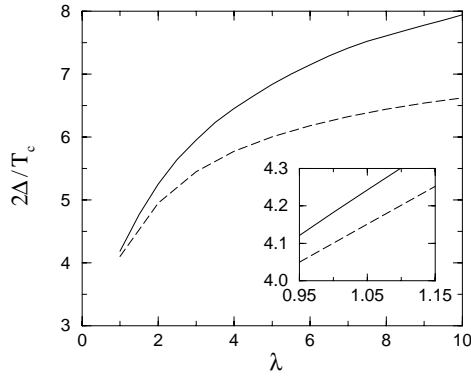


Fig. 1. Plot of $2\Delta/T_c$ (solid line) and $2\Delta_0/T_c$ (dashed line) as function of λ for an Einstein phonon spectrum and $\mu = 0$. In inset, a zoom of the region around $2\Delta/T_c = 4.2$.

where Ω_{\max} is the maximum phonon frequency. The physical properties of the superconducting state depend on μ^* rather than μ or ω_c [24]. In the numerical solution of equations (1, 2) we have set $\omega_c = 5\Omega_{\max}$. Larger values of ω_c do not modify the results and we have checked that different choices of ω_c , although providing different values of μ as expected, lead to the same μ^* via equation (5).

The quantities we want to extract from the ME equations (1) and (2) are the critical temperature T_c , the zero temperature superconducting gap Δ and the carbon isotope coefficient α_C . To achieve this, we must first choose the input quantities $\alpha^2F(\Omega)$ and μ (or μ^*). Of course, the electron-phonon coupling λ and the logarithmic phonon frequency Ω_{\ln} follows directly from a given Eliashberg function $\alpha^2F(\Omega)$ via equations (3-4). Our aim is to find for which values of λ , Ω_{\ln} and μ^* the ME equations have $T_c = 30$ K, $\alpha_C = 0.21$, and $2\Delta/T_c = 4.2 \pm 0.2$ as solutions. We solve numerically equations (1-2) to obtain the critical temperature T_c and the zero-temperature ‘‘Matsubara’’ gap $\Delta_0 = \lim_{T \rightarrow 0} \Delta(i\omega_{n=0})$.

The physical gap $\Delta(T)$ can be obtained from $\Delta(i\omega_n)$ via the analytical continuation on the real-axis [25] and through the relation

$$\Delta(T) = \text{Re} [\Delta(\omega = \Delta(T), T)]. \quad (6)$$

In order to quantify the discrepancy between Δ and Δ_0 , in Figure 1 the physical and Matsubara gaps are plotted as function of λ for a Einstein phonon model with $\mu = 0$. The enhancement of Δ with respect to Δ_0 is essentially driven by the size of the gap itself. An enlargement of the region relevant for Rb₃C₆₀ ($2\Delta/T_c \simeq 4.2$) is shown in inset of Figure 1. The discrepancy is of order of 2%, from $2\Delta_0/T_c \simeq 4.10$ to $2\Delta/T_c \simeq 4.18$. The total effect is in any case less than the experimental error of Δ in Rb₃C₆₀ [18]. Numerical solutions of Eliashberg equations in imaginary-axis therefore provide a quite good determination even of the physical gap Δ within the experimental accuracy available for Rb₃C₆₀. Note that the above discussion holds true even in the presence of Coulomb repulsion and for generic $\alpha^2F(\Omega)$. As we have pointed out, discrepancies between Δ_0 and Δ are essentially related

to the size of Δ , and therefore to $2\Delta/T_c$. The physical gap can be quite small, leading to weak-intermediate coupling phenomenology, even for large values of λ when the electron-phonon coupling is balanced by a strong Coulomb repulsion, as is the case for fullerene compounds [1].

Finally, the carbon isotope coefficient α_C , defined by

$$\alpha_C = -\frac{M_C}{\Delta M_C} \frac{\Delta T_c}{T_c}, \quad (7)$$

is numerically evaluated by solving the ME equations (1) and (2) for two values of the carbon mass: M_C and $M_C + \Delta M_C$. For a single component material, it can be shown that isotope substitution enters the ME equations only through a scaling factor in the frequency dependence of the Eliashberg function, namely [21, 26]:

$$\alpha^2F(\Omega) \equiv \mathcal{F}(\sqrt{M}\Omega), \quad (8)$$

where M is the element mass. In a two-component system, like Rb₃C₆₀, the electron-phonon spectral function $\alpha^2F(\Omega)$ contains in principle mixed phonon modes involving C-C, Rb-Rb and C-Rb displacements. The corresponding contributions to $\alpha^2F(\Omega)$ scale therefore in different ways with isotope substitution, and one should deal with partial isotope effects [21, 26]. However, inter-molecular modes involving the alkali ions appear to couple negligibly to electrons in A₃C₆₀ systems. Evidence for this conclusion comes from the negligible effect on T_c upon isotope substitution of the alkali ions [27], implying that the electron-phonon spectral function $\alpha^2F(\Omega)$ does not contain Rb-phonon modes. In addition, the dependence of T_c on the lattice parameter is identical both by applying pressure and by chemical substitution of the alkali atoms [28]. This result points out the marginal role played by alkali atoms on superconductivity: they mainly tune the lattice constant by interspacing the buckyballs molecules and provide charge carriers in the conduction band. But they do not effectively couple to electrons. Based on this experimental evidence, we assume the Eliashberg function $\alpha^2F(\Omega)$ is determined only by carbon modes. In this case, using of equation (8) is perfectly justified.

3 Numerical analysis

We are now in the position to analyze the experimental situation of Rb₃C₆₀. We solve numerically the ME equations for different shapes of $\alpha^2F(\Omega)$ with the constraints given by the measured data of Rb₃C₆₀. For the Eliashberg function $\alpha^2F(\Omega)$ we use i) a single δ -peak (Einstein spectrum, model I), ii) a broad spectrum defined by a rectangular function (model II), and iii) a broad (rectangular) spectrum with an additional low frequency contribution describing the coupling to the inter-molecular modes (model III).

3.1 Model I: Einstein phonon spectrum

As a particularly simple but representative case we first consider a δ -peaked spectrum describing a single Einstein

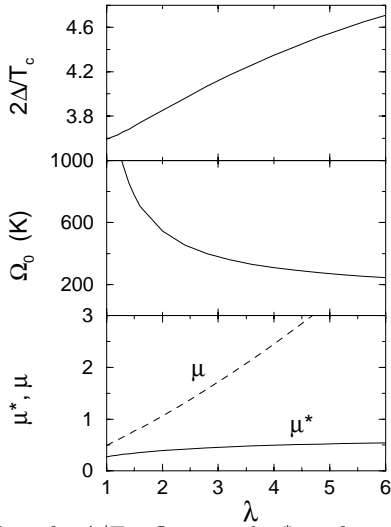


Fig. 2. Plot of $2\Delta/T_c$, Ω_0 , μ and μ^* as functions of λ as obtained by the numerical solutions of equations (1-2) with an Einstein phonon spectrum and with the conditions $T_c = 30$ K and $\alpha_C = 0.21$.

phonon with frequency Ω_0 and electron-phonon coupling constant λ :

$$\alpha^2 F(\Omega) = \frac{\lambda \Omega_0}{2} \delta(\Omega - \Omega_0). \quad (9)$$

The use of a single δ -function $\alpha^2 F(\Omega)$ makes the ME equations to be characterized just by the three microscopic parameters λ , Ω_0 and μ . Once the critical temperature $T_c = 30$ K and the isotope coefficient $\alpha_C = 0.21$ are fixed, this permits to obtain a one-to-one correspondence between the value of the ratio $2\Delta/T_c$ and a set of λ , Ω_0 , μ . The numerical results are shown in Figure 2 where we plot also the pseudopotential μ^* obtained from the calculated μ via equation (5).

The experimental ratio $2\Delta/T_c = 4.2 \pm 0.2$, together with $T_c = 30$ K and $\alpha_C = 0.21$, is obtained by an electron-phonon coupling $\lambda = 3.33_{-0.79}^{+0.90}$, an Einstein phonon $\Omega_0 = \Omega_{\text{ln}} = 350_{-52}^{+84}$ K, bare and screened Coulomb repulsions respectively $\mu = 1.95_{-0.54}^{+0.68}$ and $\mu^* = 0.47_{-0.04}^{+0.03}$, where the error bars result from the experimental uncertainty of $2\Delta/T_c$ [29]. We note that the obtained value of Ω_{ln} is compatible with the low-frequency intra-molecular modes[30] and that $\mu^* \sim 0.4 - 0.5$ is close to the most accurate theoretical estimations [31,32]. However, $\lambda = 3.33_{-0.79}^{+0.90}$ largely exceeds $\lambda \simeq 1$ which is the estimation most commonly found in literature [1]. More importantly, as we show later, the value we have found is too large to prevent lattice instabilities and to ensure the validity of Migdal's theorem. This result does not rely on the specific shape of $\alpha^2 F(\Omega)$. As we show below, different shapes of $\alpha^2 F(\Omega)$ lead to similar results in terms of λ , Ω_{ln} and μ^* .

3.2 Model II: rectangular phonon spectrum

Let us consider now the case of a spectral function with a finite width. To this end, we schematize $\alpha^2 F(\Omega)$ as a

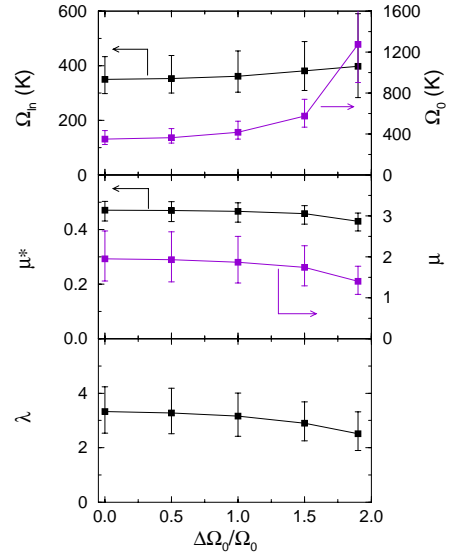


Fig. 3. Plot of λ , μ^* , Ω_{ln} (left side axes) and Ω_0 and μ (right side axes) as function of the broadening of the phonon spectrum $\Delta\Omega_0/\Omega_0$. T_c , α and $2\Delta/T_c$ are fixed to their experimental values.

rectangle centered at Ω_0 and having width $\Delta\Omega_0$. By using equation (3), $\alpha^2 F(\Omega)$ can therefore be written as:

$$\alpha^2 F(\Omega) = \frac{\lambda \theta(\Omega - \Omega_0 + \Delta\Omega_0/2) \theta(\Omega_0 + \Delta\Omega_0/2 - \Omega)}{2 \ln |(\Omega_0 + \Delta\Omega_0/2)/(\Omega_0 - \Delta\Omega_0/2)|}, \quad (10)$$

where θ is the Heaviside step function. The quantity $\Delta\Omega_0/\Omega_0$ parametrizes the finite width: for $\Delta\Omega_0/\Omega_0 \rightarrow 0$ the single Einstein phonon case (model I) is recovered, while the limit $\Delta\Omega_0/\Omega_0 \rightarrow 2$ corresponds to a constant $\alpha^2 F(\Omega)$ ranging from 0 to $2\Omega_0$. This latter case should be considered merely as a mathematical limit with no physical relevance since, as $\Omega \rightarrow 0$, $\alpha^2 F(\Omega)$ should always vanish. The characteristic quantities λ and Ω_{ln} are determined as usual from equations (3) and (4). Note that Ω_{ln} does not coincide with Ω_0 as in the Einstein model, but it is actually given by:

$$\Omega_{\text{ln}} = \left[\Omega_0^2 - \left(\frac{\Delta\Omega_0}{2} \right)^2 \right]^{1/2}. \quad (11)$$

Hence, Ω_{ln} is always smaller than Ω_0 and the equality $\Omega_{\text{ln}} = \Omega_0$ holds true only in the limit $\Delta\Omega_0/\Omega_0 \rightarrow 0$.

The effects of the finite width of the electron-phonon spectrum are shown in Figure 3, where the quantities λ , μ^* , Ω_{ln} , as well as Ω_0 and μ , obtained by requiring $T_c = 30$ K, $\alpha_C = 0.21$, $2\Delta/T_c = 4.2 \pm 0.2$, are plotted as function of the parameter $\Delta\Omega_0/\Omega_0$. The error bars correspond to the experimental uncertainty on $2\Delta/T_c$. From the analysis of Figure 3 some important remarks can be stated. First of all, we see that λ , μ^* and Ω_{ln} have only a weak dependence on the phonon spectrum width: this sustains the idea that T_c , α_C , and $2\Delta/T_c$ depend essentially only on the ‘‘McMillan’’ parameters λ , μ^* and Ω_{ln} regardless of the particular shape of $\alpha^2 F(\Omega)$. Moreover, it shows

also a lower bound for λ ($\lambda > 2$), which, although lower than the Einstein phonon case, is still outside the range of validity of Migdal-Eliashberg theory. Note that values of $\Delta\Omega_0/\Omega_0 > 1.9$ represent solutions with phonon spectra exceeding ~ 2300 K, which is the largest intramolecular phonon frequency [1,30], so that they are solutions not compatible with the real materials.

Further results can be deduced from Figure 3. In fact, intramolecular phonons in Rb₃C₆₀ extends in a range of energies $393 \text{ K} < \Omega < 2266 \text{ K}$ [1,30]. If we assume that all these phonons couple with equal strength to the electrons, then this situation would correspond to $\Omega_0 \simeq 1330 \text{ K}$ and $\Delta\Omega_0/\Omega_0 \simeq 1.4$. However, from Figure 3, $\Delta\Omega_0/\Omega_0 = 1.4$ corresponds to a phonon spectrum centered at $\Omega_0 \simeq 550 \text{ K}$, which is much lower than $\Omega_0 \simeq 1330 \text{ K}$. Furthermore, if we keep only $T_c = 30 \text{ K}$ and $\alpha_C = 0.21$ fixed, then for $\Omega_0 = 1330 \text{ K}$ and $\Delta\Omega_0/\Omega_0 = 1.4$ we find $2\Delta/T_c \simeq 3.7$. Again, this limiting situation is incompatible with the experimental data of Rb₃C₆₀.

3.3 Model III: rectangular spectrum plus inter-molecular modes

In the past, the issue of determining if intermolecular or intramolecular phonon modes are more responsible for the superconductivity phenomenon in fullerenes has been widely debated. Although an active role of alkali-C₆₀ phonons has been ruled out by the zero alkali isotope effect [27], intermolecular buckyball modes can in principle play a not negligible role in the electron-phonon coupling. Indeed, numerical calculations indicate that the intramolecular phonons couple relatively strongly to the conduction electrons [7,8,33–36], but a contribution from very low-frequency intermolecular modes (librations) has been claimed to provide a better fit to some experimental data [6]. In literature, there are examples of numerical calculations which favour [37] or disfavour [31,38,35] an important contribution of the intermolecular modes to the total λ .

In this section we consider the effects of an eventual intermolecular contribution to the total electron-phonon coupling. We schematize this contribution by adding a low-frequency part to the rectangular model of $\alpha^2F(\Omega)$ studied above. We do not distinguish between libration (of typical energy 50 K [6]), and acoustic C₆₀-C₆₀ modes (of frequency up to ~ 90 – 100 K [39]), and treat all the intermolecular couplings as a continuum ranging from $\Omega = 0$ to $\Omega = \Omega_{\text{inter}}$, where we set $\Omega_{\text{inter}} = 100 \text{ K}$ as the maximum intermolecular frequency. The overall shape of this low-frequency part is of secondary importance, the only condition is that it should vanish as $\Omega \rightarrow 0$ (this ensures that the intermolecular contribution of λ is finite, see Eq. (3)). We have therefore chosen the following expression for the total $\alpha^2F(\Omega)$:

$$\alpha^2F(\Omega) = \begin{cases} A_{\text{inter}} \Omega & 0 \leq \Omega \leq \Omega_{\text{inter}} \\ A_{\text{intra}} \left(\Omega_0 - \frac{\Delta\Omega_0}{2} \leq \Omega \leq \Omega_0 + \frac{\Delta\Omega_0}{2} \right) \end{cases}, \quad (12)$$

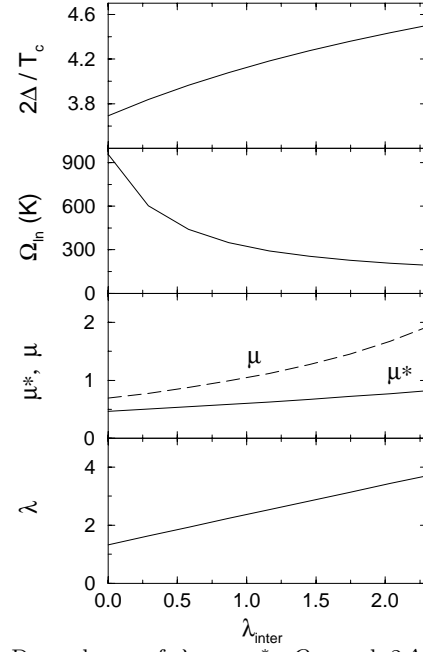


Fig. 4. Dependence of λ , μ , μ^* , Ω_{in} and $2\Delta/T_c$ on the intermolecular electron-phonon coupling λ_{inter} keeping fixed $T_c = 30 \text{ K}$ and $\alpha = 0.21$.

where, from equation (3), A_{inter} and A_{intra} are related respectively to the intermolecular and intramolecular electron-phonon coupling constants, λ_{inter} and λ_{intra} , as:

$$A_{\text{inter}} = \frac{\lambda_{\text{inter}}}{2\Omega_{\text{inter}}}, \quad (13)$$

and

$$A_{\text{intra}} = \frac{\lambda_{\text{intra}}}{2 \ln |(\Omega_0 + \Delta\Omega_0/2)/(\Omega_0 - \Delta\Omega_0/2)|}. \quad (14)$$

Moreover, from equation (4), the logarithmic frequency is:

$$\Omega_{\text{in}} = \left(\frac{\Omega_{\text{inter}}}{e} \right)^{\frac{\lambda_{\text{inter}}}{\lambda}} \left[\Omega_0^2 - \left(\frac{\Delta\Omega_0}{2} \right)^2 \right]^{\frac{\lambda_{\text{intra}}}{2\lambda}}, \quad (15)$$

where $\lambda = \lambda_{\text{inter}} + \lambda_{\text{intra}}$ is the total electron-phonon coupling. In this model, the coupling to the intermolecular phonons is modulated just by λ_{inter} , while Ω_{inter} is kept fixed at 100 K. Of course, for $\lambda_{\text{inter}} = 0$ the present model reduces to the previous model II where only intramolecular modes are taken into account.

Let us start by considering the case in which all the intramolecular phonons ($393 \text{ K} < \Omega < 2266 \text{ K}$, which corresponds to $\Omega_0 = 1330 \text{ K}$ and $\Delta\Omega_0/\Omega_0 = 1.4$) couple with the same weight to the electrons. We have seen before that for this limiting case there is no solution compatible with the experimental data of Rb₃C₆₀. By switching on the intermolecular electron-phonon coupling, however, it is now possible to find a solution which reproduces all the experimental values of T_c , α_C and $2\Delta/T_c$. The behaviour of $2\Delta/T_c$, together with Ω_{in} , μ , μ^* , and the total electron-phonon coupling λ , for fixed $T_c = 30 \text{ K}$ and $\alpha_C = 0.21$, as function of λ_{inter} is plotted in Figure 4.

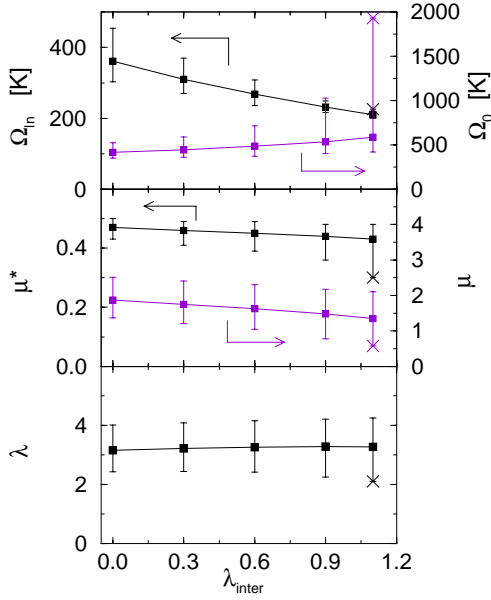


Fig. 5. Dependence of λ , μ , μ^* , Ω_{ln} and Ω_0 on the intermolecular electron-phonon coupling λ_{inter} . All the data have been obtained by requiring $T_c = 30$ K, $\alpha_C = 0.21$, and $2\Delta/T_c = 4.2 \pm 0.2$ with the exception of the results for $\lambda_{\text{inter}} = 1.1$ where the lowest value of $2\Delta/T_c$ has been set equal to 4.04 (marked by a cross).

For $\lambda_{\text{inter}} = 0$ we again find $2\Delta/T_c \simeq 3.7$, while $2\Delta/T_c = 4.2 \pm 0.2$ is obtained for $\lambda_{\text{inter}} = 1.47^{+0.80}_{-0.63}$ which corresponds to $\lambda = 2.85^{+0.83}_{-0.65}$, $\mu = 0.90^{+0.14}_{-0.10}$, $\mu^* = 0.37^{+0.02}_{-0.02}$ and $\Omega_{\text{ln}} = 178^{+99}_{-50}$ K. Although now a solution exists for $\lambda_{\text{inter}} \neq 0$, the corresponding values of λ , Ω_{ln} , and μ^* are of the same order of those extracted by the previous model I and model II.

Given $\lambda_{\text{inter}} \neq 0$, we have also studied the effect of the broadening of the intramolecular modes by using different values of $\Delta\Omega_0$. For a given $\Delta\Omega_0/\Omega_0$, the frequency Ω_0 is adjusted as function of λ_{inter} to reproduce $T_c = 30$ K, $\alpha_C = 0.21$, and $2\Delta/T_c = 4.2 \pm 0.2$. The results for $\Delta\Omega_0/\Omega_0 = 1$ are shown in Figure 5. The smaller range of intramolecular phonons leads to solutions for all intermolecular couplings up to $\lambda_{\text{inter}} = 0.9$. For $\lambda_{\text{inter}} = 1.1$ the error bars of Ω_0 becomes so large that the maximum phonon frequency $\Omega_{\text{max}} = \Omega_0 + \Delta\Omega_0/2$ exceeds the highest possible intramolecular phonon energy (2266 K). In particular, for $2\Delta/T_c = 4.04$ we have obtained $\Omega_0 = 1930$ K (marked by a cross in Fig. 5) which corresponds to $\Omega_{\text{max}} = 2895$ K. The value of Ω_0 for $2\Delta/T_c = 4.0$ would be even higher but too computing demanding to evaluate exactly.

For $\Delta\Omega_0/\Omega_0 = 0$ (Einstein phonon plus intermolecular contribution) there are solutions also at higher values of λ_{inter} , but for $\lambda_{\text{inter}} < 0.9$ the resulting λ , μ^* , and Ω_{ln} nearly exactly overlap with those of Figure 5. Hence, compared to the case in which all the intramolecular phonons participate to the coupling ($\Delta\Omega_0/\Omega_0 = 1.4$

and $\Omega_0 = 1330$ K, for which we have found $\lambda = 2.85^{+0.83}_{-0.65}$), lower values of $\Delta\Omega_0/\Omega_0$ tend to give higher values of λ .

4 Breakdown of the adiabatic hypothesis

We summarize in Table 1 the main results obtained by solving the ME equations (1) and (2) under the different models of the electron-phonon spectral function $\alpha^2F(\Omega)$ defined in Sections 3.1–3.3. For model II and model III we report the results which give only the lower values of λ ($\Delta\Omega_0/\Omega_0 = 1.9$ for model II and $\Delta\Omega_0/\Omega_0 = 1.4$, $\Omega_0 = 1330$ K, and $\lambda_{\text{inter}} = 1.47^{+0.8}_{-0.63}$ for model III).

Table 1. Summary of the numerical solutions of the ME equations for $T_c = 30$ K, $\alpha_C = 0.21$ and $2\Delta/T_c = 4.2 \pm 0.2$. For Model II and Model III we report only the set of values which defines lower limits of λ .

	$\Omega_{\text{ln}}[\text{K}]$	μ^*	λ
Model I	350^{+84}_{-52}	$0.47^{+0.03}_{-0.04}$	$3.33^{+0.90}_{-0.79}$
Model II	$< 398^{+193}_{-115}$	$> 0.43^{+0.03}_{-0.04}$	$> 2.51^{+0.81}_{-0.61}$
Model III	$> 178^{+99}_{-50}$	$> 0.37^{+0.02}_{-0.02}$	$> 2.85^{+0.83}_{-0.65}$

The main result which can be extracted from Table 1 is that, independently of the particular form of $\alpha^2F(\Omega)$ considered, the experimental data of Rb_3C_{60} can be solutions of the ME equations only for very large values of λ . Considering that model I and the lower limits of model II and model III reported in Table 1 correspond to quite extreme situations, we estimate $\lambda \simeq 3 \pm 0.8$ as the most plausible value for more realistic shapes of $\alpha^2F(\Omega)$.

Let us examine now the consequences of this result and the consistency with the whole ME framework. A first crucial point is that such high values of the electron-phonon coupling exceed the maximum allowed λ compatible with the lattice stability. Perturbative calculations of the phonon propagator show that for $\lambda \rightarrow 1$ the phonon frequencies at small momenta are renormalized to zero [40], while recent calculations on the Holstein model predict the breakdown of the ME expansion at $\lambda > 1.25$ [41]. For real materials, it is argued that $\lambda \simeq 1.5$ is a good estimate of the maximum electron-phonon coupling compatible with lattice stability [42]. Note moreover that, even for λ well below the criterion of lattice stability, the system could undergo other kinds of instabilities, like charge-density-waves, which would prevent superconductivity.

In addition to the problem concerning the lattice stability, the results obtained in the last section, when analyzed together with the band structure of Rb₃C₆₀, lead to a serious inconsistency with respect to the validity of Migdal's theorem [2]. The use of equations (1) and (2) implicitly assumes the adiabatic hypothesis according to which $E_F \gg \Omega_{\text{ph}}$, where Ω_{ph} is the typical phonon frequency and E_F is the Fermi energy. In general, the adiabatic hypothesis ensures that the electron-phonon vertex corrections, absent in the ME equation, can be neglected [2]. In fact, according to Migdal, the order of magnitude of the vertex corrections is at least

$$P = 2 \int d\Omega \frac{\alpha^2 F(\Omega)}{E_F} = \lambda \frac{\Omega_{\text{ph}}}{E_F}, \quad (16)$$

where $\Omega_{\text{ph}} = \frac{2}{\lambda} \int d\Omega \alpha^2 F(\Omega)$ [43]. Note however that the adiabatic condition $E_F \gg \Omega_{\text{ph}}$ does not automatically give $P \ll 1$ since $P \sim 1$ could be obtained for $\lambda \gg 1$. Hence, our results are consistent with the ME theory if both Ω_{ph}/E_F and P are negligible.

The electronic band structure of the fullerenes is given by a set of very narrow subbands of width $W \sim 0.5$ eV separated from each other by gaps of order $U \sim 0.5$ eV or larger [1]. For the A₃C₆₀ compounds the conduction t_{1u} subband is half-filled by electrons. Due to coupling to the phonons, the conduction electrons experience both intra- and inter-band scatterings. However, the inter-band electron-phonon couplings have only a negligible effect on superconductivity because they involve transitions of order $W + U \simeq 1$ eV or larger [7]. The relevant bandwidth is thus that of the t_{1u} conduction band and the corresponding Fermi energy is $E_F = W/2 \simeq 0.25$ eV = 2900 K. This value should be compared with the characteristic phonon frequency scale.

According to (16), in the case of an Einstein phonon spectrum (model I) the average phonon frequency Ω_{ph} reduces to Ω_0 . From the previous results of Section 3.1 we obtain therefore an adiabatic ratio $\Omega_{\text{ph}}/E_F = 0.12^{+0.03}_{-0.02}$, which is moderately nonadiabatic. However, the large value of λ reported in Table 1 leads to an important contribution of the vertex corrections, as estimated by equation (16), with a magnitude $P = 0.40^{+0.03}_{-0.02}$ far from to be negligible. The effects on P and Ω_{ph}/E_F of the broadening (model II) and of the inclusion of inter-molecular modes (model III) in $\alpha^2 F(\Omega)$ are reported in Figures 6 and 7, respectively. For model II, the explicit expression of P can be obtained from equations (10) and (16) and reduces to:

$$P = \frac{\lambda}{\ln\left(\frac{\Omega_0 + \Delta\Omega_0/2}{\Omega_0 - \Delta\Omega_0/2}\right)} \frac{\Delta\Omega_0}{E_F}, \quad (\text{model II}) \quad (17)$$

while for model III, equation (12), P becomes:

$$P = \frac{\lambda_{\text{inter}}}{2} \frac{\Omega_{\text{inter}}}{E_F} + \frac{\lambda - \lambda_{\text{inter}}}{\ln\left(\frac{\Omega_0 + \Delta\Omega_0/2}{\Omega_0 - \Delta\Omega_0/2}\right)} \frac{\Delta\Omega_0}{E_F} \quad (\text{model III}). \quad (18)$$

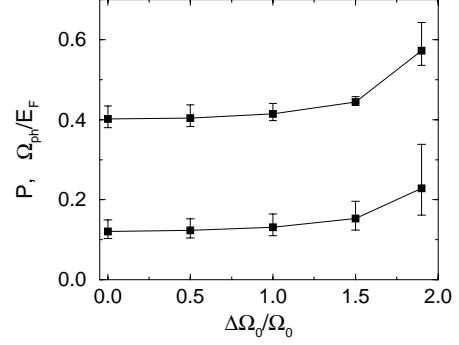


Fig. 6. Adiabatic ratio Ω_{ph}/E_F (lower line) and Migdal's parameter $P = \lambda\Omega_{\text{ph}}/E_F$ (upper line) as function of the broadening of the phonon spectrum in model II.

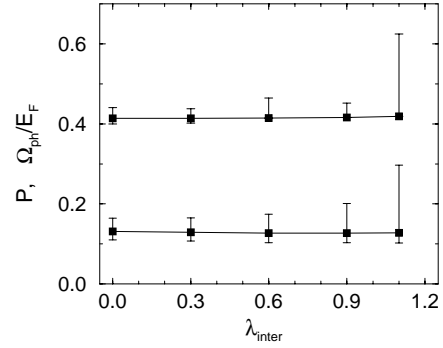


Fig. 7. Adiabatic ratio Ω_{ph}/E_F (lower line) and Migdal's parameter $P = \lambda\Omega_{\text{ph}}/E_F$ (upper line) as function of the inter-molecular electron-phonon coupling in model III ($\Delta\Omega_0/\Omega_0 = 1.0$).

From Figure 6 it is apparent that the broadening affects only weakly the Einstein phonon results, $\Delta\Omega_0/\Omega_0 = 0$, at least for $\Delta\Omega_0/\Omega_0 \leq 1$. For larger values of $\Delta\Omega_0/\Omega_0$ both P and Ω_{ph}/E_F increase signaling an even stronger violation of the adiabatic hypothesis and of Migdal's theorem. Switching on the low frequency inter-molecular couplings, Figure 7, does not modify appreciably the results of Figure 6. In fact, the effect of non zero values of λ_{inter} is to shift Ω_0 to slightly higher frequencies than for $\lambda_{\text{inter}} = 0$ (see Fig. 5), leading to an almost λ_{inter} -independent Ω_{ph} .

Summarizing the results obtained for $E_F = 0.25$ eV, we conclude that $\Omega_{\text{ph}}/E_F \gtrsim 0.12$ and $P \gtrsim 0.4$ independently of the shape of $\alpha^2 F(\Omega)$. Hence, the experimental data of Rb₃C₆₀ are not consistent with the ME theory since both the adiabatic hypothesis, $\Omega_{\text{ph}}/E_F \ll 1$, and Migdal's theorem, $P \ll 1$, are violated.

How much this result depends on the precise determination of the superconducting gap size? All over our analysis we have considered an experimental uncertainty $2\Delta/T_c = 4.2 \pm 0.2$ and we have shown that within this error bars any attempt to describe the experimental data breaks down the adiabatic hypothesis. However, recent measurements by surface-sensitive techniques seem to point towards a BCS-like value of the reduced gap $2\Delta/T_c \simeq 3.53$ [44], and

one could question the validity of our conclusions for such a small value of Δ . However, the violation of ME theory is even stronger in this case. As shown in Figure 2 for an Einstein phonon spectrum (model I), BCS-like values of Δ need coupling with extremely high phonon energies in order to reproduce $T_c = 30$ K and $\alpha_C = 0.21$. In particular, $2\Delta/T_c = 3.6$ implies $\Omega_0 = 1350$ K, corresponding to an adiabatic ratio $\Omega_{\text{ph}}/E_F \simeq 0.46$ and to a Migdal's parameter $P \simeq 0.49$. The failure of ME theory is even more drastic if broader spectra (models II and III) are considered. Indeed, as discussed in Section 3, in these cases a lowest value $2\Delta/T_c \simeq 3.7$ is obtained and a BCS-like gap $2\Delta/T_c = 3.53$, together with $T_c = 30$ K and $\alpha_C = 0.21$, is incompatible with the ME framework.

5 Discussion and conclusions

The critical analysis of the experimental data carried on in the previous sections has pointed out the inconsistency of the standard ME theory for Rb_3C_{60} . We address now the origin of such inconsistency in the hypothesis that phonons are still the mediators of superconductivity in Rb_3C_{60} . To this end, let us consider some existing theoretical calculations of the coupling of the t_{1u} electrons to the H_g intra-molecular phonon modes. Each phonon mode has frequency Ω_i , $i = 1, \dots, 8$, and couples to the t_{1u} electrons via $V_i = \lambda_i/N_0$, N_0 being the electron density of states per spin at the Fermi level. In Figure 8 we show a collection of data taken from various calculations [7, 8, 33–36], and for each set of data we have estimated the corresponding adiabatic parameter Ω_{ph}/E_F where, from equation (16),

$$\Omega_{\text{ph}} = \frac{2}{\lambda} \int d\Omega \alpha^2 F(\Omega) = \frac{1}{V} \sum_{i=1}^8 \Omega_i V_i, \quad (19)$$

and $V = \sum_i V_i$. The data refer to different schemes including tight-binding, LDA, *ab initio* etc., and the error bars stem from the uncertainty in the calculated t_{1u} bandwidth (we have assumed $E_F = 0.25 \pm 0.05$ eV).

The important point of Figure 8 is that, despite of the large spread of the values of λ/N_0 , all these calculations agree in estimating the adiabatic parameter Ω_{ph}/E_F to be larger than about 0.4, so that Migdal's theorem breaks down and the whole ME framework is invalidated. Of course, the reason for such high values of Ω_{ph}/E_F stems from the fact that, independently of details, the H_g phonons have energies ranging from 30 meV to 200 meV while the conduction t_{1u} electron band has a width of only $W = 0.4 - 0.6$ eV.

With the exception of few cases (see for example Ref. [35]) the problem concerning the non-validity of the adiabatic hypothesis is ignored or, at best, underestimated and the numerical results are often claimed to provide a strong evidence that, after all, the fullerene compounds are standard ME superconductors [45]. Our opinion is instead that such numerical calculations show quite clearly an evident nonadiabaticity of the electron-phonon interaction for which the ME framework is completely inadequate. Hence, a correct description of the superconducting

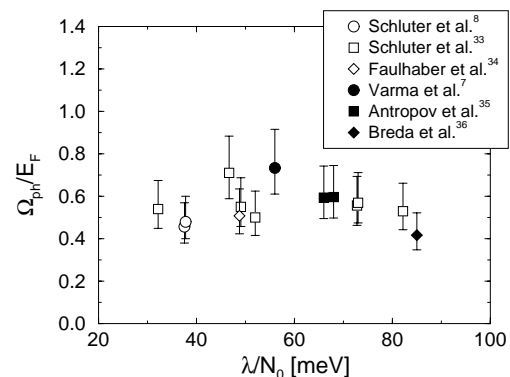


Fig. 8. Adiabatic parameter Ω_{ph}/E_F extracted from various calculations of the intramolecular electron-phonon interaction in fullerenes.

state in fullerenes should be formulated in such a way that Ω_{ph}/E_F can assume values larger than zero for which the electron-phonon vertex corrections, as well as finite-band effects, must be included from the start. As by-products of the very small value of E_F , also non-constant density of state effects and strong electron correlations may play a role in the superconducting properties of fullerenes. However, these effects alone can hardly explain the high values of T_c while, under favourable circumstances, the electron-phonon vertex corrections can effectively enhance the pairing interaction [46], leading to an increase of T_c for values of λ lower than those needed in the ME theory [47].

It would be therefore interesting to test whether and for which parameter values a theory generalized beyond Migdal's theorem can describe the experimental data of Rb_3C_{60} . The accomplishment of this task is outside the scope of this work. However as shown in reference [23], preliminary results suggest a positive role of the nonadiabatic electron-phonon effects. For example, while in the adiabatic ME equations a $\lambda = 1 - 4$ is needed in order to reproduce $T_c = 30$ K and $\alpha_C = 0.21$ for realistic values of phonon frequencies $300 \text{ K} \lesssim \Omega_{\text{ph}} \lesssim 1500 - 1800 \text{ K}$, a much more reasonable $\lambda < 1$ is needed in the nonadiabatic theory of superconductivity where first nonadiabatic corrections are taken into account [23].

These results are quite interesting since they suggest that the experimental data of Rb_3C_{60} could be explained by values of λ much closer to those of the intercalated compounds of graphite ($\lambda \sim 0.3$). This is an important remark because the intramolecular phonons in C_{60} stem from the carbon-carbon bonds just as the highest phonon modes of graphite. In this perspective, the large discrepancy between the superconducting critical temperature in graphite intercalated compounds ($T_c \sim 0.2$ K) and in fullerenes would come from the difference of the electronic structures. Graphite compounds have large Fermi energies locating these materials in the adiabatic regime where ME equations actually hold, while the small values of E_F of the fullerenes give rise to the opening of nonadiabatic channels enhancing the pairing.

References

1. O. Gunnarsson, Rev. Mod. Phys. **69**, 575 (1997).
2. A.B. Migdal, Zh. Eksp. Teor. Fiz. **34**, 1438 (1958) [Sov. Phys. JETP **7**, 996 (1958)].
3. G.M. Eliashberg, Zh. Eksp. Teor. Fiz. **38**, 966 (1960) [Sov. Phys. JETP **11**, 696 (1960)].
4. T.T.M. Palstra, O. Zhou, Y. Iwasa, P.E. Sulevski, R.M. Fleming, B.R. Zegarski, Solid. State Comm. **93**, 327 (1995).
5. F.C. Zhang, M. Ogata, T.M. Rice, Phys. Rev. Lett. **67**, 3452 (1991).
6. I.I. Mazin, O.V. Dolgov, A. Golubov, S.V. Shulga, Phys. Rev. B **47**, 538 (1993).
7. C.M. Varma, J. Zaanen, K. Raghavachari, Science **254**, 989 (1991).
8. M. Schluter, M. Lannoo, M. Needeles, G.A. Baraff, D. Tománek, Phys. Rev. Lett. **68**, 526 (1992).
9. M. Côté, J.C. Grossman, M.L. Cohen, S.G. Louie, Phys. Rev. Lett. **81**, 697 (1998).
10. Y.J. Uemura *et al.*, Nature **352**, 605 (1991).
11. S. Chakravarty, S. Kivelson, Europhys. Lett. **16**, 751 (1991).
12. Y. Iwasa, H. Shimoda, T.T.M. Palstra, Y. Maniwa, O. Zhou, T. Mitani, Phys. Rev. B **53**, R8836 (1996).
13. O. Gunnarsson, E. Koch, R.M. Martin, Phys. Rev. B **54**, R11026 (1996).
14. T. Yildirim, L. Barbedette, J.E. Fischer, C.L. Lin, J. Robert, P. Petit, T.T.M. Palstra, Phys. Rev. Lett. **77**, 167 (1996).
15. S.K. Watson, K. Allen, D.W. Denlinger, F. Hellman, Phys. Rev. B **55**, 3866 (1997).
16. J.H. Schön, Ch. Kloc, B. Batlogg, Nature **408**, 549 (2000).
17. M.S. Fuhrer, K. Cherrey, A. Zettl, M.L. Cohen, V.H. Crespi, Phys. Rev. Lett. **83**, 404 (1999).
18. D. Koller, M.C. Martin, L. Mihály, G. Mihály, G. Oszlányi, G. Baumgartner, L. Forró, Phys. Rev. Lett. **77**, 4082 (1996).
19. R. Tycko, G. Dabbagh, M.J. Rosseinsky, D.W. Murphy, A.P. Ramirez, R.M. Fleming, Phys. Rev. Lett. **68**, 1912 (1992).
20. Chun Gu *et al.*, Phys. Rev. B **50**, 16566 (1994).
21. J.P. Carbotte, Rev. Mod. Phys. **62**, 1027 (1990).
22. R.D. Parks, *Superconductivity* (Marcel Dekker Inc., New York, 1969), p. 126.
23. E. Cappelluti, C. Grimaldi, L. Pietronero, S. Strässler, Phys. Rev. Lett. **85**, 4771 (2000).
24. R. Combescot, Phys. Rev. B **42**, 7810 (1990).
25. F. Marsiglio, M. Schossmann, J.P. Carbotte, Phys. Rev. B **37**, 4965 (1988).
26. D. Rainer, F.J. Culetto, Phys. Rev. B **19**, 2540 (1979).
27. T.W. Ebbesen *et al.*, Physica C **203**, 163 (1992); B. Burk, V.H. Crespi, A. Zettl, M.L. Cohen, Phys. Rev. Lett. **72**, 3706 (1994).
28. R.M. Fleming *et al.*, Nature **352**, 787 (1991).
29. Here and in the following, we neglect the error bars in α_C since they add only a small fraction of the uncertainty of $2\Delta/T_c$ to the values of λ , Ω_{in} , and μ^* .
30. A.F. Hebard, Phys. Today **45**, No. 11, 26 (1992).
31. O. Gunnarsson, G. Zwicknagl, Phys. Rev. Lett. **69**, 957 (1992).
32. E. Koch, O. Gunnarsson, R.M. Martin, Phys. Rev. Lett. **83**, 620 (1999).
33. M. Schluter, M. Lannoo, M. Needeles, G.A. Baraff, D. Tománek, J. Phys. Chem. Solids **53**, 1473 (1992).
34. J.C.R. Faulhaber, D.Y.K. Ko, P.R. Briddon, Phys. Rev. B **48**, 661 (1993).
35. V.P. Antropov, O. Gunnarsson, A.I. Liechtenstein, Phys. Rev. B **48**, 7651 (1993).
36. N. Breda, R.A. Broglia, G. Coló, H.E. Roman, F. Alasia, G. Onida, V. Ponomarev, E. Vigezzi, Chem. Phys. Lett. **286**, 350 (1998).
37. G. Chen, Y. Guo, N. Karasawa, W.A. Goddard III, Phys. Rev. B **48**, 13959 (1993).
38. W.E. Pickett, D.A. Papaconstantopoulos, M.R. Pederson, S.C. Erwin, J. Superconductivity **7**, 651 (1994).
39. Y. Wang, D. Tománek, G.F. Bertsch, Phys. Rev. B **44**, 6562 (1991).
40. A.A. Abrikosov, L.P. Gorkov, I.E. Dzyaloshinski, *Method of Quantum Field Theory in Statistical Physics* (Dover, New York, 1963).
41. P. Benedetti, R. Zeyher, Phys. Rev. B **58**, 14320 (1998).
42. P.W. Anderson, C.C. You, in *Highlights of Condensed Matter Theory, Proc. of the Int. School of Physics "Enrico Fermi", LXXXXIX*, edited by F. Bassani, M. Tosi, (North-Holland, 1985), p. 767.
43. Note that in equation (16) enters the averaged phonon frequency Ω_{ph} rather than the logarithmic frequency Ω_{ln} . They coincide in case of a single δ -peak spectrum, while in general $\Omega_{\text{ln}} \leq \Omega_{\text{ph}}$.
44. R. Hesper, L.H. Tjeng, A. Heeres, G.A. Sawatzky, Phys. Rev. Lett. **85**, 1970 (2000).
45. In reference [17] *ab initio* local density calculations have led to $\Omega_{\text{ln}} = 1390$ K and this result has been used to extract $\lambda \simeq 0.9$ from a solution of the ME equations constrained to have $T_c = 30$ K and $\alpha_C = 0.21$. We find that, from the data of reference [17] and by using $E_F \simeq 0.25$ eV, $\Omega_{\text{ln}}/E_F \simeq 0.48$ and $\lambda\Omega_{\text{ln}}/E_F \simeq 0.43$. So, also from the data of reference [17] we find that Migdal's theorem is violated.
46. L. Pietronero, S. Strässler, C. Grimaldi, Phys. Rev. B **52**, 10516 (1995); C. Grimaldi, L. Pietronero, S. Strässler, Phys. Rev. B **52**, 10530 (1995); *ibid.* Phys. Rev. Lett. **75**, 1158 (1995).
47. P. Benedetti, C. Grimaldi, L. Pietronero, G. Varelogiannis, Europhys. Lett. **28**, 351 (1994).